PLOS ONE

RESEARCH ARTICLE

Effects of prenatal low protein and postnatal high fat diets on visceral adipose tissue macrophage phenotypes and IL-6 expression in Sprague Dawley rat offspring

Linglin Xie[1,2]*, Ke Zhang[3,4], Dane Rasmussen[2], Junpeng Wang[5], Dayong Wu[5], James N. Roemmich[6], Amy Bundy[6], W. Thomas Johnson[6], Kate Claycombe[6]*

1 Department of Nutrition and Food Sciences, Texas A&M University, College Station, Texas, United States of America, **2** Department of Basic Sciences, School of Medicine and Health Sciences, University of North Dakota, Grand Forks, North Dakota, United States of America, **3** Department of Pathology, School of Medicine and Health Sciences, University of North Dakota, Grand Forks, North Dakota, United States of America, **4** ND INBRE Bioinformatics Core, University of North Dakota, Grand Forks, North Dakota, United States of America, **5** Jean Mayer USDA Human Nutrition Research Center on Aging at Tufts University, Boston, Massachusetts, United States of America, **6** USDA Agricultural Research Service, Grand Forks Human Nutrition Research Center, Grand Forks, North Dakota, United States of America

* linglin.xie@tamu.edu (LX); kate.claycombe@ars.usda.gov (KJC)

Citation: Xie L, Zhang K, Rasmussen D, Wang J, Wu D, Roemmich JN, et al. (2017) Effects of prenatal low protein and postnatal high fat diets on visceral adipose tissue macrophage phenotypes and IL-6 expression in Sprague Dawley rat offspring. PLoS ONE 12(1): e0169581. doi:10.1371/journal.pone.0169581

Editor: Vanessa Souza-Mello, State University of Rio de Janeiro, BRAZIL

Received: September 9, 2016

Accepted: December 19, 2016

Published: January 31, 2017

Data Availability Statement: All relevant data are within the paper.

Funding: This project was supported by grants from the National Institutes of Health (NIH-1R15HL117238 to author LX, National Center for Research Resources, 5P20RR016471-12/8 P20 GM103442-12 to authors LX and KZ) and the American Heart Association (13SDG14650009 to author LX). This work was also supported by USDA Agricultural Research Service Project

Abstract

Adipose tissue macrophages (ATM) are implicated in adipose tissue inflammation and obesity-related insulin resistance. Maternal low protein models result in fetal programming of obesity. The study aims to answer whether maternal undernutrition by protein restriction affects the ATM M1 or M2 phenotype under postnatal high fat diet in F1 offspring. Using a rat model of prenatal low protein (LP, 8% protein) diet followed by a postnatal high fat energy diet (HE, 45% fat) or low fat normal energy diet (NE, 10% fat) for 12 weeks, we investigated the effects of these diets on adiposity, programming of the offspring ATM phenotype, and the associated inflammatory response in adipose tissue. Fat mass in newborn and 12-week old LP fed offspring was lower than that of normal protein (20%; NP) fed offspring; however, the adipose tissue growth rate was higher compared to the NP fed offspring. While LP did not affect the number of $CD68^+$ or $CD206^+$ cells in adipose tissue of NE offspring, it attenuated the number of these cells in offspring fed HE. In offspring fed HE, LP offspring had a lower percentage of $CD11c^+CD206^+$ ATMs, whose abundancy was correlated with the size of the adipocytes. Noteworthy, similar to HE treatment, LP increased gene expression of *IL-6* within ATMs. Two-way ANOVA showed an interaction of prenatal LP and postnatal HE on *IL-6* and *IL-1β* transcription. Overall, both LP and HE diets impact ATM phenotype by affecting the ratio of $CD11c^+CD206^+$ ATMs and the expression of *IL-6*.

#3062-51000-052-00D to author KJC and by the USDA National Institute of Food and Agriculture, [Hatch] project [1010406] to author LX.

Competing Interests: The authors have declared that no competing interests exist.

Abbreviations: ANOVA, analysis of variance; ATM, macrophages; CLS, crown like structure; H&E, Haematoxylin Eosin; HE, high fat/energy diet (45% fat); IUGR, induced intrauterine growth restriction; LBW, low birth weight; LP, low protein (8%); NE, normal fat/energy diet (20% fat); NP, normal protein (20% protein); PBS, phosphate-buffered saline; SEM, standard error of the mean; SVC, Stromal Vascular Cell.

Introduction

Epidemiologic studies have shown that low birth weight (LBW) is associated with increased incidence of obesity, coronary heart disease, type 2 diabetes and metabolic syndrome [1–5]. A well-established cause of LBW is maternal under nutrition–induced intrauterine growth restriction (IUGR) [6, 7]. As proposed in the thrifty phenotype hypothesis [8], maternal under-nutrition slows fetal growth. This enhances the fetus' ability to survive by reserving nutrients for developing critical organs, such as brain, kidney and heart, at the expense of adipose, muscular and skeletal tissue development. However, when these offspring are exposed to over-nutrition, the greater ability to efficiently store nutrients results in obesity in later life [9–11]. In agreement with this hypothesis, IUGR results in subsequent postnatal catch-up growth and development of obesity [12, 13]. Maternal low protein models of fetal programming have been widely used to investigate the mechanisms linking maternal nutrition with F1 obesity [14–16]. A common trait in the F1 offspring is an age-related loss of glucose tolerance and development of insulin resistance [17–20]. In order to understand the underlying mechanisms for the glucose intolerance associated with IUGR, studies have focused on the alterations in insulin secretion and action that occur during catch-up growth [21].

The obesity epidemic has resulted in an explosion of obesity-related health problems, including insulin resistance and type II diabetes. The chronic low-grade inflammation that occurs within the adipose tissue of obese subjects contributes to pathogenesis of insulin resistance [22]. Macrophages are the major adipose tissue-resident immune cell types involved in the development of chronic inflammation [22–24]. The adipose tissue of obese mice has a 2- to 5-fold increase in macrophage infiltration, along with higher systemic levels of macrophage-secreted inflammatory cytokines [22].

Macrophages show heterogeneity in their function depending on the resident microenvironment. Classically activated or M1 macrophages ($CD11c^+$) produce pro-inflammatory cytokines (e.g. TNF-α, IL-1β and IL-6) and are the predominant type of adipose tissue macrophages (ATMs) in dietary-induced obese (DIO) humans and animals [25, 26]. M1 macrophages are sub-divided into M1a and M1b types based on the absence or presence of CD206, respectively [27]. Alternatively activated or M2 macrophages ($CD11c^-CD206^+$) secret anti-inflammatory cytokines (e.g. IL-4, IL-10 and IL-1 receptor antagonist) and are a dominant population of ATM in lean mice [26, 28, 29]. In contrast to the progress in defining the role of ATM in the pathogenesis of obesity-related insulin resistance, little is known of how maternal undernutrition influences ATM phenotypes of offspring consuming normal or high energy diets.

Using a rat model of a prenatal low protein (LP, 8% protein) diet followed by a normal or a postnatal high fat energy diet (HE, 45% fat) for 12 weeks, effects of these diets on programming of the offspring ATM phenotype were investigated in the current study. We found that maternal LP did not affect the number of CD68+ or CD206+ cells in adipose tissue of NE offspring, but increased the gene expression of IL-6 and IL-1β. However, maternal LP diet interact with postnatal HE diet interacts on the catch up growth and the enlargement of the offspring adipocyte, which further correlates with the ATM phenotype.

Materials and methods

Study design

Two month old obese-prone Sprague-Dawley male and female rats were purchased from Charles River (Wilmington, MA) and maintained on a chow diet for 2 weeks prior to the start of experiment diets. Twelve female Sprague Dawley rats were placed on either the control

Table 1. Prenatal low and normal protein diet composition.

	Normal Protein (NP)		Low Protein (LP)	
Ingredient	g	kcal	g	kcal
Casein	200	800	80	320
L-cysteine	3	12	3	12
Corn Starch	310	1240	390.82	1563.3
Maltodextrin	35	140	35	140
Sucrose	297.5	1190	337.91	1351.6
Cellulose	50		50	
Soybean oil	25	225	25	225
Lard	20	180	20	180
$CaCO_3$	12.5		7.27	
$CaHPO_4$			4	
Mineral mix	35		35	
Vitamin mix	10	40	10	40
Choline bitartrate	2		2	
Total	1000	3827	1000	3827
	wt%	kcal%	wt%	kcal%
Protein	20.3	21.22	8.3	8.66
Carbohydrate	67.24	67.26	79.36	79.83
Fat	4.5	10.58	4.5	10.57

doi:10.1371/journal.pone.0169581.t001

(NP, 20% protein, n = 12 litters) or low-protein (LP, 8% protein, n = 12 litters) diet 2 days after conception and remained on this diet throughout gestation and lactation. The females were mated for 2 days. Pregnancy was confirmed when plugs were found. Pregnant females were then placed in a single cage and weighed weekly for 3 week gestational period. At birth, litter size and birth weight were recorded and offspring (F1) were randomly culled to 8 pups (4 male, 4 female). We used 4 male pups from each dam for further experiments. At weaning, one-half of the male offspring born to dams fed LP were placed on a diet containing an energy density of 3.84 kcal/g (10% fat energy, 70% carbohydrate energy, and 20% protein energy; hence referred to as the NE—normal energy diet), the other half were given a diet containing 4.73 kcal/g (45% fat energy, 20% carbohydrate energy, and 20% protein energy; hence referred to as the HE—high energy diet) (Table 1). Because rats fed HE ate less, these diets had higher concentrations of vitamins, minerals, and protein such that these nutrients in the HE diet were equivalent to the NE diet on a per kcal basis (Table 2). Offspring were divided into four groups: NP+NE, LP+NE, NP+HE, and LP+HE. Offspring were maintained on these diets for 12 weeks. The food efficiency was determined by dividing body weight gain of each experimental mice by the total energy intake.

All animals were caged in a controlled environment with a 12-hour light, 12-hour dark cycle and received pathogen-free water. At the end of 12-week postnatal diets, rats were injected with xylazine (Rompon, Moboay Inc., Shawnee, KS) and ketamine (Ketaset, Aveco Inc., Fort Dodge, IA) and sacrificed by exsanguinations according to the USDA ARS animal care and use committee guidelines.

The animal use and care protocol was approved by USDA Agricultural Research Service Animal Care and Use Committee (Permit Number: Claycombe-Prog04). Rats were injected with xylazine (Rompon, Moboay) and ketamine (Ketaset, Aveco) and killed by exsanguination, and all efforts were made to minimize suffering.

Table 2. Postnatal normal and high fat diet composition.

	Normal Protein (NP)		Low Protein (LP)	
Ingredient	g	kcal	g	kcal
Casein	200	800	80	320
L-cysteine	3	12	3	12
Corn Starch	315	1260		
Maltodextrin	35	140	125	500
Sucrose	350	1400	215	860
Cellulose	50		50	
Soybean oil	25	225	25	225
Lard	20	180	20	180
$CaCO_3$	12.5		12.5	
Mineral mix	35		35	
Vitamin mix	10	40	10	40
Choline bitartrate	2		2	
Total	1057.5	4057	857.5	4057
	3.84 kcal/g		4.73 kcal/g	
	wt%	kcal%	wt%	kcal%
Protein	19.20	20.01	23.67	20.01
Carbohydrate	66.19	69.12	43.13	33.62
Fat	4.26	9.98	23.91	45.48

doi:10.1371/journal.pone.0169581.t002

Antibodies

Mouse anti-rat CD11b/c PerCP-eFluor® 710 (Cat#46–0110) and its isotype control (Cat#46–4724) for flow cytometry were purchased from eBioscience (San Diego, CA). Anti-Mouse Ig APC (Cat# 550826) for flow cytometry was purchased from BD bioscience (San Jose, CA) and Donkey Anti-Rabbit IgG PE (Cat#12-4739-81) was from eBioscience (San Diego, CA). Anti-rat CD68 FITC (Cat#SM1550F) for flow cytometry was from Acris-antibodies (San Diego, CA). Rabbit anti-rat CD206 (Mannose Receptor antibody) (Cat#ab64693), mouse anti-rat CD11c (Cat#ab11029) and mouse anti-rat CD68 (Cat#ab53444) for immunohistochemical staining were from Abcam (Cambridge, MA).

EchoMRI measurements of body composition

Whole body composition (fat mass, lean mass, and total body water) was determined biweekly without any sedation using nuclear magnetic resonance technology with EchoMRI700™ instrument (Echo Medical Systems, Houston, TX) during the 12 week postnatal diet period.

Stromal Vascular Cell (SVC) isolation and FACS analysis

Epididymal fat pads were weighed, rinsed 3 times in phosphate-buffered saline (PBS), and the SVCs were isolated as described previously [30]. SVCs were immunostained with primary antibodies for 30 min at 4˚C followed by incubation with fluorescent-bounded secondary antibody for another 30 min at 4˚C in dark. SVCs were analyzed using an Accuri C6 flow cytometer (BD Accuri Cytometers, Ann Arbor, MI), and data were analyzed with FlowJo 7.6 software (Treestar Inc., Ashland, OR).

Adipose tissue analysis

Experimental offspring mice were euthanized by CO_2 inhalation. Visceral white adipose tissue was immediately collected and fixed in 10% formalin/PBS. The tissue was embedded in paraffin blocks after processing and was cut into 5-μm-thick slices using a TC-2 tissue sectioner (Sorvall Instruments). Tissue slices were mounted onto positive pre-charged glass slides to ensure optimal adhesion. CD68 (Acris-antibodies, San Diego, CA), CD206 (Abcam, Cambridge, MA) and CD11c (Abcam, Cambridge, MA) were immunostained using a VECTASTAIN Elite Avidin/Biotin-Complex (ABC) kit for mouse IgG or a VECTASTAIN Elite ABC kit for rabbit IgG (Vector Laboratory). Staining of the tissue was visualized under an Olympus BH-2 microscope and pictures were taken using a Leica M165FC camera and Leica Application Suit V3 was used for picture processing. The number of positive cells per 1000 adipocytes in each staining section was blindly counted. The average of the five counts was used for data analysis. Adipocyte diameter was measured using Image J software. Two hundred cells were randomly counted in each sample. The adipocytes of five animals from each group were counted. An average diameter was recorded for each animal.

Isolation of $CD68^+$ macrophages from SVCs

SVCs were treated with 1% Tween-20 PBS for 30 minutes at room temperature. Then SVCs were incubated with anti-rat CD68 FITC (Acris-antibodies, San Diego, CA) for 30 minutes at 4˚C in dark and washed with Magnetic Cell Separation (MACS) buffer (Miltenyi Biotec Inc., Auburn, CA). SVCs were then incubated with anti-FITC MicroBeads (Miltenyi Biotec Inc., Auburn, CA) for 15 minutes at 4˚C in dark and washed twice with MACS buffer. The pellets were re-suspended in 500 μl MACS buffer and flow through MS columns (Miltenyi Biotec Inc., Auburn, CA) according to the manufacturer's manual. The FITC MicroBeads bound $CD68^+$ cells were collected for RNA extraction.

Real-time PCR

Total RNA of $CD68^+$ cells from SVCs was extracted using Invitrogen Trizol reagent. cDNA was synthesized using Qiagen RT^2 First Strand Kit (Qiagen, Valencia, CA). Primers were designed as listed in Table 3. Real time PCR was performed using an ABI Prism 7500 PCR system (Applied Biosystems, Foster City, CA). The ΔCT values were used for statistical analysis for real time-PCR experiments. The standard deviation of the fold change in gene expression for real time-PCR data was derived by the delta method [31].

Statistical analysis

The normality of data was ensured using Shapiro-Wilk test. Differences between the groups were analyzed using Fishers' Least Significant Difference (LSD) test such that the multiple

Table 3. Primers used for RT-PCR experiment.

Gene	forward primer	reverse primer
IL-6	5′-ggtttgccgagtagacctca-3′	5′-gtggctaaggaccaagacca-3′
IL-1β	5′- aaagaaggtgcttgggtcct-3′	5′- caggaaggcagtgtcactca-3′
MCP-1	5′- ccgactcattgggatcatct-3′	5′- tagcatccacgtgctgtctc-3′
Arg1	5′- gacatccacaaaggccagat-3′	5′- tatcggagcgcctttctcta-3′
IL-10	5′-tgggaagtgggtgcagttat-3′	5′- gctcagcactgctatgttgc-3′

doi:10.1371/journal.pone.0169581.t003

comparisons between groups were taken into account. Fisher's LSD test was performed by first carrying out one-way analysis of variance (ANOVA) for all four treatment groups and then conducting two-group pairwise t-tests only for outcomes showing statistical significance in the ANOVA tests. Because two factors, maternal (LP vs NP) and postnatal (HE vs NE), were involved in the experimental design, two-way ANOVA was used to assess the main effects and the interaction between the two factors. The correlation between the ratio of M1b cells to M1 cells and the sizes of adipose cells were analyzed using ordinary least squares regression analysis. The M1b ratio data were logarithm transformed prior to analysis because Breusch-Pagan test found that the original ratios did not fit a linear model. All analyses were carried out using SAS® JMP software and R statistical programming language. The significance level of statistical test was defined as $P<0.05$. Data in graphs are presented as mean ± SEM and sample size n. Bars bearing different letters indicated significant difference between the bars ($P<0.05$).

Results

Prenatal LP offspring had lower adipose tissue mass and higher adipose tissue growth rate compared to NP offspring

LP offspring had lower body and adipose tissue weights at weaning compared to the NP offspring (Fig 1A and 1D). While these prenatal LP-induced differences remained significant at postnatal week 12, offspring fed the postnatal HE diets had greater body weights and body fat mass than the NE rats, regardless of prenatal diet (Fig 1B and 1E). However, when calculated as fold change, LP (vs. NP) increased body weight gain independent of postnatal diets, while HE diets only increased body weight gain in LP offspring, but not in NP offspring (Fig 1C). The prenatal LP and postnatal HE synergistically increased the weight gain and fat gain of offspring, with LP+HE rats having the largest catch-up weight gain and fat gain compared to NP +HE rats (Fig 1C and 1F).

Offspring fed postnatal HE had larger visceral adipocytes compared to offspring fed NE. However, the prenatal LP diet diminished this effect of HE because LP+HE rats had smaller adipocytes compared to NP+HE rats (Fig 1G and 1H). Since feed efficiency (body weight gain/energy intake) is an important contributing factor in adipose tissue weight gain, we therefore calculated the feed efficiency of the offspring. The results showed that feed efficiency were significantly increased in LP offspring, but not in the HE offspring, although feed efficiency in NP+HE offspring was slightly higher than NE+NP offspring. Clearly, this result does not explain the adipose tissue weight gain (Fig 1I).

Prenatal LP prevented $CD68^+$ and $CD206^+$ cell infiltration in visceral adipose tissue of DIO rats

We have summarized the macrophage markers used in our study for M1, M2 and subtypes of M1 macrophages in Table 4. The number of $CD68^+$ cells in each group was normalized to the number of $CD68^+$ macrophages in the NP+NE group. More ATM were observed in HE offspring compared to NE offspring regardless of prenatal diet (HE vs. NE on NP diet: 2.44±0.05 vs. 1.00±0.11, $P<0.01$; HE vs. NE on LP diet: 0.89±0.27 vs. 1.53±0.03, $P<0.05$). The prenatal LP diet decreased the number of $CD68^+$ ATM only in offspring fed HE diets (Fig 2A–2I) (LP vs. NP on HE diet: 2.44±0.05 vs. 1.53±0.03, $P<0.01$).

$CD11c^+$ cells (Fig 3A–3H) and $CD68^+$ cells (Fig 2A–2H) were highly recruited to the crown like structure (CLS), but much more scattered in non-CLS regions of rats from HE groups. Interestingly, $CD68^+$ or $CD11c^+$ cells aggregate more around adipocytes in LP+NE rats than

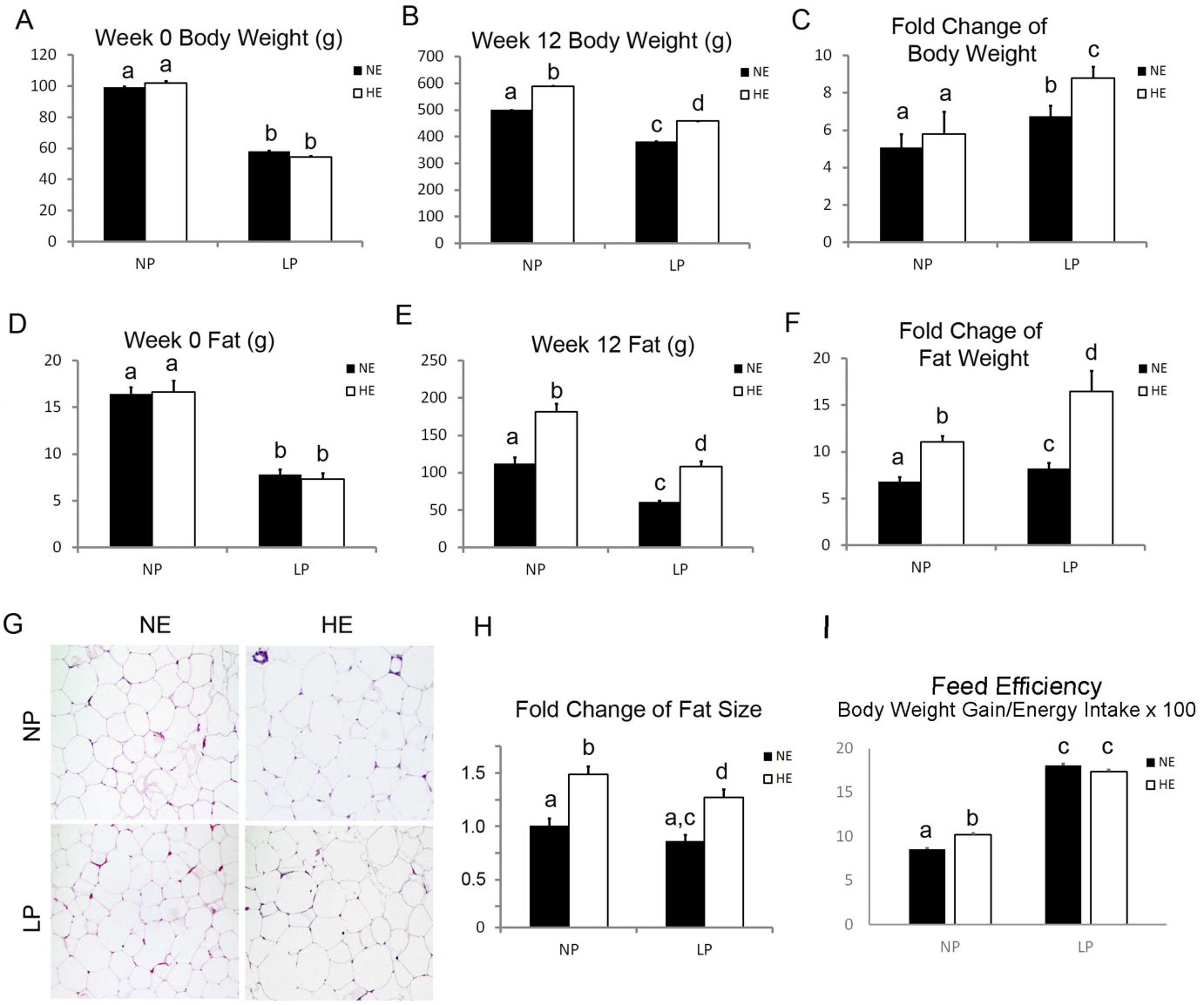

Fig 1. Prenatal LP offspring had reduced adipose tissue mass but significantly increased adipose tissue gain. A and B). Body weight of the experimental rats was measured at week 0 (weaning weight) and week 12. Data are presented as mean ± SEM, n = 9–12. C). Body weight change was calculated by dividing the body weight (g) and then subtracted one at week 12 by the weaning body weight (g). Data are presented as mean ± SEM, n = 9–12. D-E) Body fat mass was measure by EchoMRI at week 0 (weaning weight) and week 12. Data are presented as mean ± SEM, n = 9–12. F) Body fat change was calculated by dividing the fat weight (g) at week 12 by the weaning fat weight (g). Data are presented as mean ± SEM, n = 9–12. Bars bearing different letters significantly differ at P<0.05. G and H) Visceral fat tissue was collected for tissue slide sectioning and H&E staining. Eight hundred adipocytes from each rat sectioning were randomly picked up and the size was measured by ImageJ. Five rats were counted in each group. Size of the adipocytes was normalized to that of the NP+NE rats. Data are presented as mean ± SEM, n = 5. Bars bearing different letters significantly differ at P<0.05. I). The feed efficiency was calculated by "body weight gain/energy intake x100". Data are presented as mean ± SEM, n = 5. Bars bearing different letters significantly differ at P<0.05.

doi:10.1371/journal.pone.0169581.g001

in NP+NE rats. CD11c$^+$ cells were much more frequent in NP+HE rats compared to NP+NE rats (HE vs. NE on NP diet: 1.30±0.02 vs. 1.00±0.03, P<0.01). However, the difference in CD11c$^+$ cell populations between LP+HE and LP+NE rats was not significant (Fig 3R). Overall, LP did not change the number of CD11c$^+$ cells in adipose tissue. There were 21.3% more

Table 4. Identification markers used in our study to classify macrophage phenotypes.

Classification	Surface marker		
M1	CD11b/c$^+$CD11c$^+$	M1a	CD11b/c$^+$CD11c$^+$ CD206$^-$
		M1b	CD11b/c$^+$CD11c$^+$ CD206$^+$
M2	CD11b/c$^+$ CD11c$^-$CD206$^+$		

doi:10.1371/journal.pone.0169581.t004

CD206$^+$ cells in NP offspring with HE diets compared to those with NE diets (Fig 3S) (HE vs. NE on NP diet: 1.21±0.12 vs. 1.00±0.03, P<0.05). Whereas HE increased CD206$^+$ cells in NP offspring, LP decreased CD206$^+$ population in rats fed the HE diet, but not in rats fed the NE diet (Fig 3S) (LP vs. NP on HE diet: 1.21±0.12 vs. 1.03±0.04, P<0.05).

HE diet increased the percentage of M1b ATM, while LP inhibited ATM phenotype switch to M1b in rats fed with HE diets

The percentage of CD11c$^+$ cells among CD11b/c$^+$ population was not changed by either HE or LP diets (Fig 4A). There was no change in percentage of CD11c$^-$CD206$^+$ among the CD11b/c$^+$

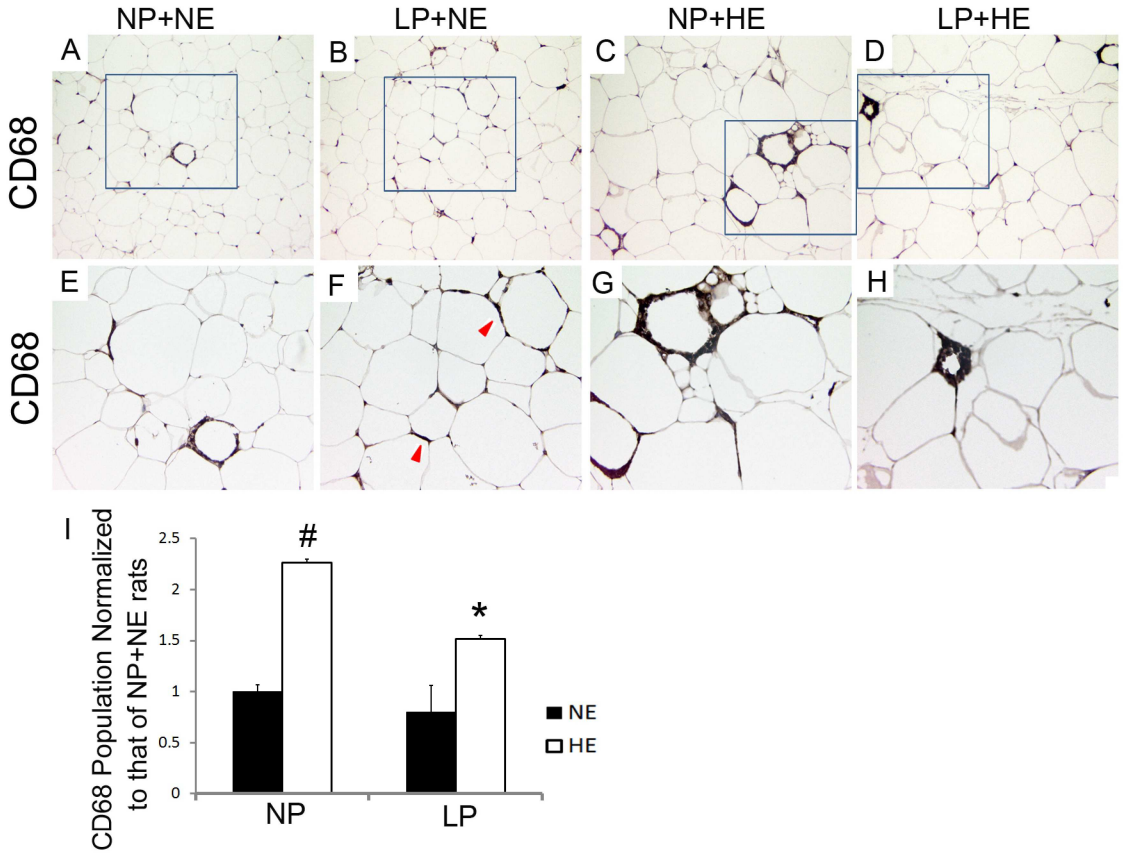

Fig 2. Prenatal LP prevented CD68$^+$ ATM infiltration triggered by HE diets. A-I) ATMs were stained with anti-CD68 antibody. The number of ATMs was counted per 1,000 adipocytes area. Three randomly selected areas were counted for each rat. Average number of the ATMs was used for further statistical analysis. Number of CD68 positive cells in each group is normalized to the number of CD68$^+$ macrophages in NP+NE group. Data are presented as mean ± SEM, n = 6–9."#" P<0.05 compared to NE; "*" P<0.05 compared to NP. E, F, G, and H are enlargements of the framed fields of A, B, C, and D, respectively. Magnificence of A-D: 200X; E-H 400X.

doi:10.1371/journal.pone.0169581.g002

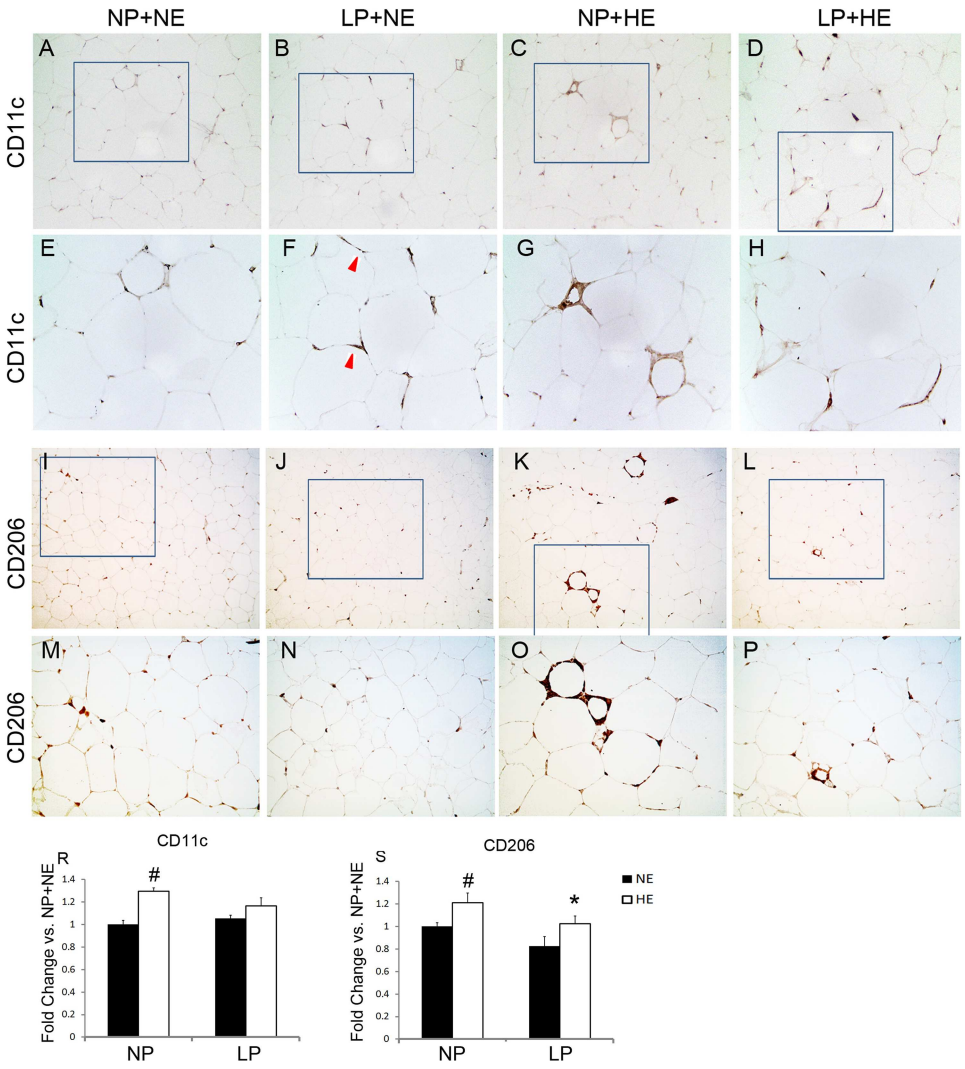

Fig 3. HE diets enhanced number of CD11c$^+$ or CD206$^+$ cells in visceral adipose tissue, while LP inhibited the increase of CD11c$^+$ or CD206$^+$ cells due to HE diets. A-H and R). Visceral adipose tissue was stained with anti-CD11c. Number of CD11c$^+$ cells was counted per 1,000 adipocytes area. Three randomly selected areas were counted for each rat. Number of CD11c positive cells in each group is normalized to the number of CD11c$^+$ macrophages in NP+NE group. Average number of the CD11c$^+$ was used for further statistical analysis. Data are presented as mean ± SEM, n = 5."#" P<0.05 compared to NE; "*" P<0.05 compared to NP. E, F, G, and H are enlargements of the framed fields of A, B, C, and D, respectively. I-P and S). Visceral adipose tissue was stained with anti-CD206. Number of CD206$^+$ cells was counted per 1,000 adipocytes area. Three randomly selected areas were counted for each rat. Number of CD206 positive cells in each group is normalized to the number of CD206$^+$ macrophages in NP+NE group. Average number of the CD206$^+$ was used for further statistical analysis. Data are presented as mean ± SEM, n = 9–12. M, N, O, and P are enlargements of the framed fields of I, J, K, and L, respectively. Magnificence of A-D and I-L: 200X; E-H and M-P 400X.

doi:10.1371/journal.pone.0169581.g003

population due to LP or HE diets (Fig 4B). The M1/M2 ratio also was not changed among all four groups (Fig 4C). However, the percentage of CD11c$^+$CD206$^+$ in total CD11c$^+$ (M1b/M1) was enhanced by HE in NP fed rats (Fig 4D) (HE vs NE on NP diet: 51.1%±0.9% vs. 28.8% ±1.7%, P<0.05). However, a prenatal LP diet blocked the increase in M1b induced by HE diets

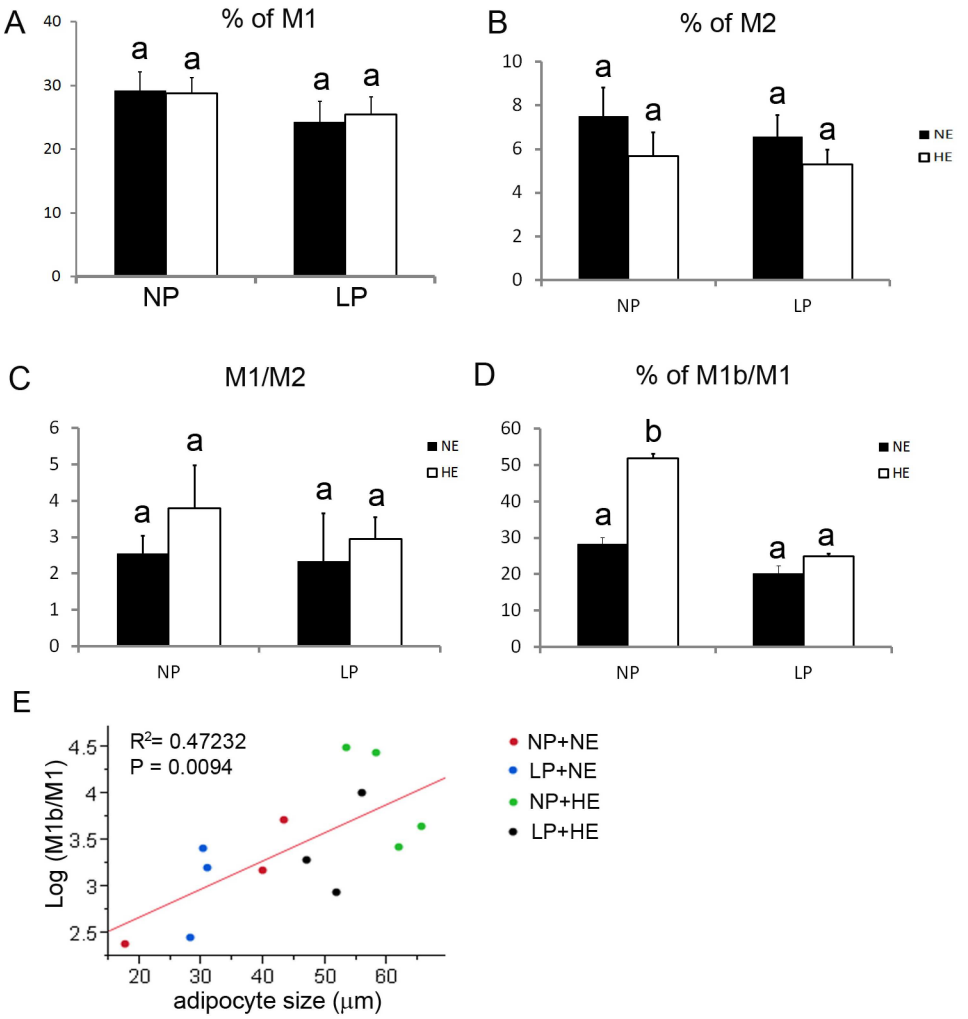

Fig 4. LP and HE impacts on ATMs plasticity. Isolated adipose tissue SVCs were stained with anti-CD11b/c PerCP-eFluor® 710, anti-CD11c PE, anti-CD206 FITC for flow cytometry analysis. The M1% (A) and the M2% (B) were measured within the CD11b/c^{+}, marker for monocytes/macrophages population. Data are presented as mean ± SEM, n = 9–12. Bars bearing different letters significantly differ at P<0.05.

doi:10.1371/journal.pone.0169581.g004

(Fig 4D, HE+NP vs. HE+LP) (LP vs NP on HE diet: 25.4%±0.7% vs. 51.1%±0.9%, P<0.01). The percentage of M1b in M1 population was associated with the size of adipocytes (Fig 4E) (R^2 = 0.47232, P = 0.0094).

Prenatal LP and postnatal HE interacted on altering IL-6 and IL-1β transcription in ATMs

There were no changes in the expression of M2 macrophage marker genes *IL-10* and *Arg-1* or in gene expression of *MCP-1* in any group, (Fig 5A–5C). Expression of *IL-6* was increased in NP+HE rats compared to NP+NE rats (Fig 5D) (HE vs. NE on NP diet: 10.0±3.8 vs. 1.0±0.04, P<0.05). *IL-6* expression was higher in LP compared to NP offspring (Fig 5D) (LP vs. NP on NE diet: 16.8±7.2 vs. 1.0±0.04, P<0.05). Surprisingly, LP combined with HE did not enhance *IL-6* expression in a synergic manner. Instead, LP partially prevented the increase in *IL-6*

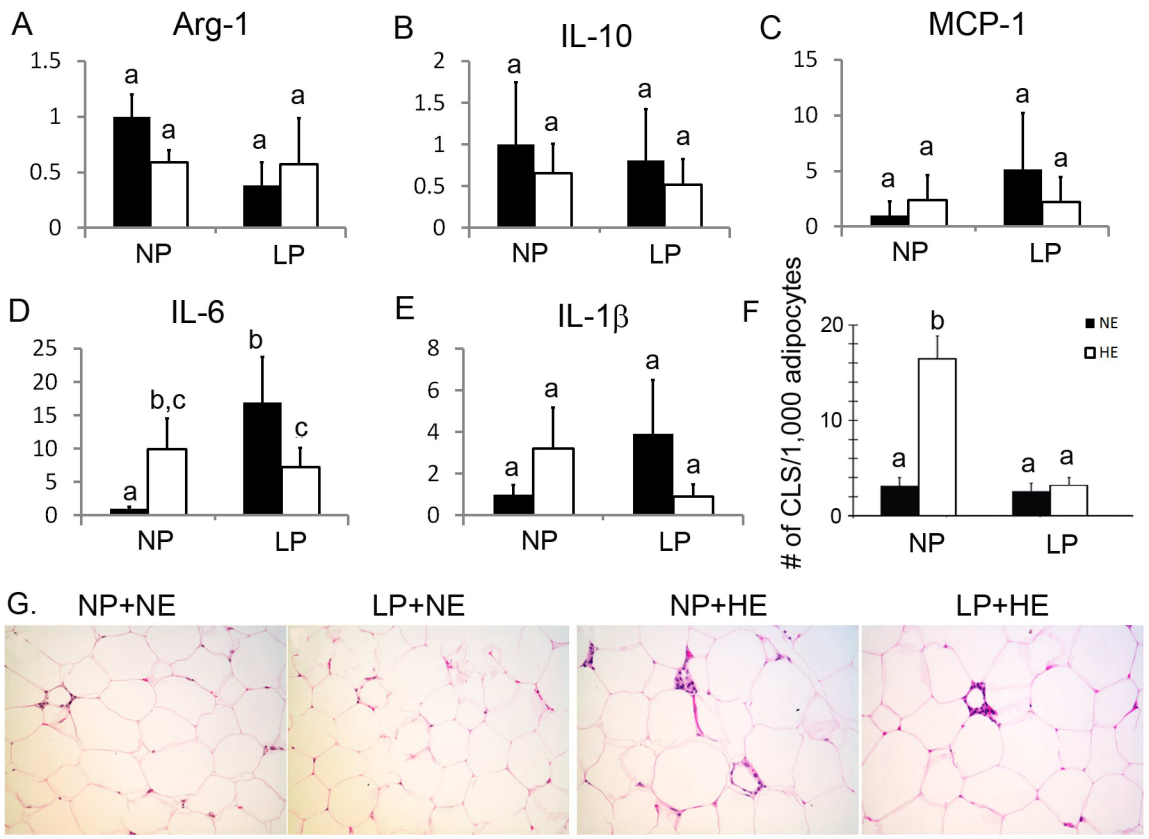

Fig 5. LP increased *IL-6* and *IL-1β* expression in isolated ATMs. A-E) Expression of *Arg-1*, *IL-10*, *MCP-1*, *IL-6* and *IL-1β* were detected by real-time PCR analysis. Data are presented as mean ± SEM, n = 3. Bars bearing different letters significantly differ at P<0.05. F and G) H&E staining on visceral adipose tissue. The number of CLS was counted per 1,000 adipocytes area. Five randomly selected areas were counted for each rat. Average number of the CLS was used for further statistical analysis. Data are presented as mean ± SEM, n = 9–12. Bars bearing different letters significantly differ at P<0.05. Magnificence of panel G is 400X.

doi:10.1371/journal.pone.0169581.g005

expression in HE rats, although *IL-6* expression still remained higher in LP+HE rats than NP +NE rats (Fig 5D) (LP vs. NP on HE diet: 16.8±7.2 vs. 7.1±2.4, P<0.05). We did not observe any transcriptional difference of *IL-1β* among all four groups (Fig 5E). However, two-way ANOVA analysis indicated that prenatal LP is a contributing factor that significantly altered the expression of *IL-1β* and *IL-6* (Table 5). In addition, the interaction evaluation by two-way ANOVA demonstrated antagonistic effect of LP and HE in regulating transcription of both *IL-6* and *IL-1β* (Table 5).

Haematoxylin Eosin (H&E) staining of visceral adipose tissue showed that CLS was more frequent in HE rats compared to NE rats (HE vs NE on NP diet, 15±2 vs. 3±1, P<0.05). While LP did not change CLS in NE rats, it decreased the number of CLS in HE rats (Fig 5F–5J). There was an interaction of LP and HE in the formation of CLS (Table 5, P < .0001).

Discussion

Adipose tissue inflammation, contributed by macrophage infiltration into the adipose tissue, is an important step in the pathogenesis of obesity-related complications. These ATM are phenotypically heterogeneous and present different plasticity in lean versus obese subjects [26]. ATM characteristics have been well described in high-fat diet-induced obesity or genetic-

Table 5. P value of Two-way ANOVA for LP and HE on ATM phenotype[a].

	HE (P value)	LP (P value)	LP × HE (P value)
IL-6	0.0003**	< .0001**	< .0001**
IL-1β	0.0048**	0.0016**	0.0043**
Ccl2	0.3276	0.0825	0.1816
IL-10	0.4826	0.7238	0.9701
Arg-1	0.4897	0.2649	0.3888
Number of $CD68^+$	< .0001**	0.4229	0.104
Number of $CD11c^+$	0.0008**	0.4644	0.0852
Number of $CD206^+$	0.0364*	0.0904	0.5771
Number of CLS	< .0001**	0.688	< .0001**

Note:

[a] The significant impacts of the two factors: postnatal HE diet and the maternal LP diet, and the interactions between these two factors on ATM phenotype and cytokine gene expression were analyzed by Two-way ANOVA.

** P<0.01,

* P<0.05

doi:10.1371/journal.pone.0169581.t005

related obesity [22, 26, 32, 33]. Previous study has reported that a low protein diet during pregnancy affects lymphocyte and complementary systems [34, 35]. However, there is limited information whether prenatal programming, affected by maternal protein restriction, changes ATM heterogeneity. It is also unknown whether maternal low protein diet and postnatal high fat diet interact to influence ATM phenotype. We reported that LP had no effect on the number of CD68+ and CD206+ in adipose tissue of NE rats, but reduced the increase of these cell numbers in offspring fed HE diet. The increase of adipose tissue CD206+CD11c+ ATMs in offspring fed HE diet was reversed by consuming a LP diet. Similar to HE treatment, LP increased *IL-6* expression in ATMs of offspring rats fed NE diets. However, this effect was diminished when offspring was fed on HE diet, which suggested an interaction between prenatal LP and postnatal HE diets on *IL-6* and *IL-1β* transcription.

Compared to a severe 4% protein [36], maternal 8% protein undernutrition diet as used in our current study do not cause significant decrease in key fetal growth factor hormone concentration alterations [36]. In addition, as shown in other studies, rat offspring exposed to 8% prenatal modest protein restricted diet do not have abnormal kidney functions or blood pressure while a more severe 5% prenatal protein restriction caused offspring kidney dysfunction and hypertension [37–41]. Therefore it is plausible 5% prenatal protein diet restriction would significantly increase the numbers of CD68+ or CD206+ cells compared to NP group adipose tissue. However, since the severe protein restriction leads to multi-organ dysfunction, the changes in plasticity of macrophages, if observed, will be more due to a compensatory or secondary effect rather than directly driven by maternal protein restriction. Thus, we choose to use a moderate protein restriction to study how prenatal and postnatal diets influence the ATM phenotype.

According to the "phenotypic switch" model of ATM, obesity leads to an accumulation of macrophages in the adipose tissue with M1-dominant phenotype, while ATM in non-obese subjects possess the M2-dominant phenotype. This is caused by direct activation of newly attracted macrophages/monocytes, rather than a phenotypic switch among resident macrophages [27, 42]. In our study, infiltration of ATM was not affected by the LP diet as evidenced by the lack of difference in the number of $CD68^+$ cells in adipose tissue. However, upon postnatal HE treatment, there were less M1b subtype ATMs (CD11c+CD206+) in F1 offspring

from the dam of maternal LP comparing to those from the maternal NP diet. Therefore, maternal LP diet interacts with postnatal HE diet to impact on the existing ATM phenotype, although prenatal LP diet may not influence the migration ability of adipose tissue monocyte/ macrophages in F1 offspring of rats.

The increased expression of *IL-6* in ATM of LP offspring suggested that prenatal LP was capable of inducing macrophage inflammation. Consistently, two-way ANOVA also indicated increased expression of *IL-1β* by maternal LP diet. Interestingly, this effect was diminished under the condition of postnatal HE, which is consistent with previous report that the expression profile of genes associated with inflammation was reduced in the visceral adipose tissue of offspring rats from a dam with maternal protein restriction [43]. These data suggested a potentially antagonistic effect of maternal protein restriction and postnatal high energy on *IL-6* and *IL-1β* expression.

However, these interesting observations seemed to suggest that the prenatal LP diet is differentially affecting ATM phenotype with or without postnatal diet. To be noted, our data demonstrated a smaller adipocyte size in LP offspring and a positive correlation between adipocyte size and M1b/M1 ratio. A relationship between adipose tissue macrophage accumulation and adipocyte size has been demonstrated in many adipose tissue depots [44]. When fat cells reach a critical size, signals are generated to promote the release of pro-inflammatory cytokines and free fatty acids (FFA) resulting in recruitment of macrophages and a switch in macrophage phenotype [32, 44] Therefore, an increase in adipocyte size might be a necessary condition for adipocytes to synthesize and release proteins that regulate ATM heterogeneity. In our study, prenatal LP significantly reduced the wean body weight and wean fat however leads to catchup growth of the body weight and body fat mass, implying a size catchup of the LP adipocytes with persistent postnatal HE diet.

The feed efficiency (body weight gain/ energy intake) is an important contributing factor in adipose tissue weight gain. Thus, we compared feed efficiency across all 4 experimental groups. Our calculation showed (data not shown) that food efficiency do not explain additional increase in adipose tissue increase in LPHF (and LPNF to a lesser extent) group suggesting possible epigenetic maternal influence in adipose tissue growth.

We therefore describe our model as follows (Fig 6). In juvenile LP+HE fed rats, despite fast growth of adipose tissue, there is a relatively lower grade of chronic inflammation in this adipose tissue than the juvenile NP+ HE offspring. This is correlated with the smaller adipocyte size, lower numbers of CLS in adipose tissue, and M1b subtype ATMs that are the major M1 subset contributing to the secretion of pro-inflammatory cytokines and insulin resistance [32]. Because prenatal LP leads to catchup growth of the body weight and adiposity[45], which might be associated with increased *Igf2* expression in LP offspring [46], it can be reasonably predicted that persistent HE diets from the juvenile stage to adult stage in LP offspring will eventually exceed the maximum capacity of adipose tissue to adapt to excess energy and lead to severe insulin resistance. The increased expression of *IL-6* in ATMs caused by LP diets will exacerbate insulin resistance in adult rats fed HE diets. This model is in consistent with previously reported studies that alterations in insulin resistance in response to LP prenatal and HE postnatal diets before and after 5 months of age [46, 47]. Extended treatment of postnatal HE diets on the same model of prenatal protein restriction in future studies will help to support the validity of this model.

In conclusion, we provide evidence that prenatal protein restriction preprogram the ATMs by increasing expression of the pro-inflammatory genes *IL-6* and *IL-1β* in ATMs. The prenatal protein restriction plays a synergic role with the postnatal high energy diet on the catch up growth and the enlargement of the adipocyte, which further correlates with the ATM plasticity and adipose tissue inflammation.

A)

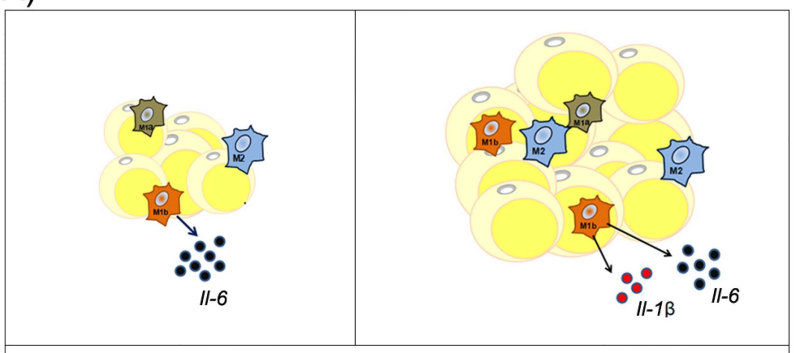

Diet Conditions			
Prenatal		**Postnatal**	
LP *vs.* **NP**	(-)Adipose size (+) Adipose tissue catch-up growth (++) MΦ *Il-6*	**HE** *vs.* **NE**	(++)Adipose size (++) MΦ recruitment (+) $CD11c^{+}$. $CD206^{+}$ (+) M1b/M1 (+) MΦ *Il-6, Il-1*β

B)

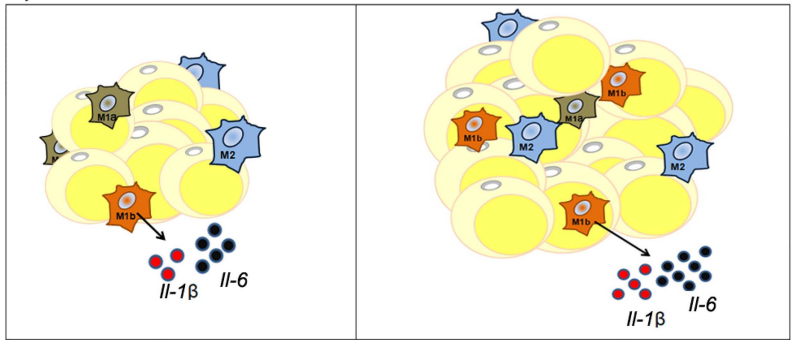

Prenatal LP combined with Postnatal HE	
Week 12	**Week 20 (Predicted)**
(+)Adipose size (+) Adipose tissue catch-up growth (+) MΦ recruitment (+) MΦ *Il-6*	(++)Adipose size (++) MΦ recruitment (++) MΦ *Il-6, Il-1*β (++) M1b/M1 (+) $CD11c^{+}$. $CD206^{+}$

Fig 6. Model of LP and HE effects on macrophage activation and plasticity. A) Prenatal LP decreases the size of adipocytes, while increases adipose tissue catch-up growth. LP by itself also inhibited *IL-6* expression in ATMs, which is independent of the adipocyte size. Postnatal HE increases the size of adipocytes, which causes the recruitment of M1, especially m1b macrophages to the adipose tissue. These ATMs expressed more *IL-6* and *IL-1β*. B) When prenatal LP diets are combined with postnatal HE diets for 12 weeks, adipocyte is enlarged but is still smaller than NP+HE rats. There is induced adipose tissue inflammation in LP+HE rats; however, they have less ATM infiltration and decreased *IL-6* in ATMs comparing to that of NP+HE rats, which were correlated with smaller size of adipocytes. Considering that LP+HE rats have largest adipose tissue-catch up growth, it is predictable that prolonged HE diets on LP offspring for 20 weeks will eventually break up the temporary balance due to significantly enlarged adipocytes.

doi:10.1371/journal.pone.0169581.g006

Acknowledgments

L.X., K.C. T.J. and J.R. designed the research; L.X., K.C., D.W., D.R. A.B. and J.W. conducted research; K.Z. did statistical analysis; L.X. and K.C. wrote the paper. L.X. and K.C. had primary responsibility for final content. All authors read and approved the final manuscript. We thank Ms. Hongyan Wang of UND forensic lab for the fat tissue processing and sectioning. We

thank Dr. Li Ning for the assistance on the IHC staining. Authors are also grateful to Dr. Eric Uthus for providing technical assistance.

Author Contributions

Conceptualization: LX KC TJ JR.

Formal analysis: KZ.

Investigation: LX KC DW DR AB JW.

Writing – review & editing: LX KC.

References

1. Andersen LG, Angquist L, Eriksson JG, Forsen T, Gamborg M, Osmond C, et al. Birth weight, childhood body mass index and risk of coronary heart disease in adults: combined historical cohort studies. PLoS One. 2010; 5(11):e14126. Epub 2010/12/03. doi: 10.1371/journal.pone.0014126 PMID: 21124730
2. Anderson SE, Gooze RA, Lemeshow S, Whitaker RC. Quality of early maternal-child relationship and risk of adolescent obesity. Pediatrics. 2012; 129(1):132–40. Epub 2011/12/28. doi: 10.1542/peds.2011-0972 PMID: 22201144
3. Meier JJ. Linking the genetics of type 2 diabetes with low birth weight: a role for prenatal islet maldevelopment? Diabetes. 2009; 58(6):1255–6. Epub 2009/05/23. doi: 10.2337/db09-0225 PMID: 19461116
4. Lindsay RS, Dabelea D, Roumain J, Hanson RL, Bennett PH, Knowler WC. Type 2 diabetes and low birth weight: the role of paternal inheritance in the association of low birth weight and diabetes. Diabetes. 2000; 49(3):445–9. Epub 2000/06/27. PMID: 10868967
5. Frankel S, Elwood P, Sweetnam P, Yarnell J, Smith GD. Birthweight, adult risk factors and incident coronary heart disease: the Caerphilly Study. Public Health. 1996; 110(3):139–43. Epub 1996/05/01. PMID: 8668758
6. Kusin JA, Kardjati S, Houtkooper JM, Renqvist UH. Energy supplementation during pregnancy and postnatal growth. Lancet. 1992; 340(8820):623–6. Epub 1992/09/12. PMID: 1355209
7. Ramachandran P. Maternal nutrition–effect on fetal growth and outcome of pregnancy. Nutr Rev. 2002; 60(5 Pt 2):S26–34. Epub 2002/05/31. PMID: 12035855
8. Hales CN, Barker DJ. Type 2 (non-insulin-dependent) diabetes mellitus: the thrifty phenotype hypothesis. Diabetologia. 1992; 35(7):595–601. Epub 1992/07/01. PMID: 1644236
9. Remacle C, Bieswal F, Reusens B. Programming of obesity and cardiovascular disease. Int J Obes Relat Metab Disord. 2004; 28 Suppl 3:S46–53. Epub 2004/11/16.
10. Ong KK, Dunger DB. Perinatal growth failure: the road to obesity, insulin resistance and cardiovascular disease in adults. Best Pract Res Clin Endocrinol Metab. 2002; 16(2):191–207. Epub 2002/06/18. doi: 10.1053/beem.2002.0195 PMID: 12064888
11. Reynolds CM, Li M, Gray C, Vickers MH. Preweaning growth hormone treatment ameliorates adipose tissue insulin resistance and inflammation in adult male offspring following maternal undernutrition. Endocrinology. 2013; 154(8):2676–86. Epub 2013/05/30. doi: 10.1210/en.2013-1146 PMID: 23715866
12. Ravelli AC, van der Meulen JH, Michels RP, Osmond C, Barker DJ, Hales CN, et al. Glucose tolerance in adults after prenatal exposure to famine. Lancet. 1998; 351(9097):173–7. Epub 1998/02/05. PMID: 9449872
13. Ravelli GP, Stein ZA, Susser MW. Obesity in young men after famine exposure in utero and early infancy. The New England journal of medicine. 1976; 295(7):349–53. Epub 1976/08/12. doi: 10.1056/NEJM197608122950701 PMID: 934222
14. Dahri S, Snoeck A, Reusens-Billen B, Remacle C, Hoet JJ. Islet function in offspring of mothers on low-protein diet during gestation. Diabetes. 1991; 40 Suppl 2:115–20. Epub 1991/12/01.
15. Gosby AK, Maloney CA, Caterson ID. Elevated insulin sensitivity in low-protein offspring rats is prevented by a high-fat diet and is associated with visceral fat. Obesity (Silver Spring). 2010; 18(8):1593–600. Epub 2009/12/19.
16. Ozanne SE, Wang CL, Coleman N, Smith GD. Altered muscle insulin sensitivity in the male offspring of protein-malnourished rats. Am J Physiol. 1996; 271(6 Pt 1):E1128–34. Epub 1996/12/01. PMID: 8997235

17. Hales CN, Desai M, Ozanne SE, Crowther NJ. Fishing in the stream of diabetes: from measuring insulin to the control of fetal organogenesis. Biochem Soc Trans. 1996; 24(2):341–50. Epub 1996/05/01. PMID: 8736760

18. Wilson MR, Hughes SJ. The effect of maternal protein deficiency during pregnancy and lactation on glucose tolerance and pancreatic islet function in adult rat offspring. J Endocrinol. 1997; 154(1):177–85. Epub 1997/07/01. PMID: 9246952

19. Poore KR, Fowden AL. The effect of birth weight on glucose tolerance in pigs at 3 and 12 months of age. Diabetologia. 2002; 45(9):1247–54. Epub 2002/09/21. doi: 10.1007/s00125-002-0849-y PMID: 12242457

20. Poore KR, Fowden AL. Insulin sensitivity in juvenile and adult Large White pigs of low and high birthweight. Diabetologia. 2004; 47(2):340–8. Epub 2004/01/15. doi: 10.1007/s00125-003-1305-3 PMID: 14722651

21. Lukaszewski MA, Mayeur S, Fajardy I, Delahaye F, Dutriez-Casteloot I, Montel V, et al. Maternal prenatal undernutrition programs adipose tissue gene expression in adult male rat offspring under high-fat diet. Am J Physiol Endocrinol Metab. 2011; 301(3):E548–59. Epub 2011/06/30. doi: 10.1152/ajpendo.00011.2011 PMID: 21712534

22. Xu H, Barnes GT, Yang Q, Tan G, Yang D, Chou CJ, et al. Chronic inflammation in fat plays a crucial role in the development of obesity-related insulin resistance. J Clin Invest. 2003; 112(12):1821–30. Epub 2003/12/18. doi: 10.1172/JCI19451 PMID: 14679177

23. Hotamisligil GS, Shargill NS, Spiegelman BM. Adipose expression of tumor necrosis factor-alpha: direct role in obesity-linked insulin resistance. Science. 1993; 259(5091):87–91. Epub 1993/01/01. PMID: 7678183

24. Ferrante AW Jr. Obesity-induced inflammation: a metabolic dialogue in the language of inflammation. J Intern Med. 2007; 262(4):408–14. Epub 2007/09/19. doi: 10.1111/j.1365-2796.2007.01852.x PMID: 17875176

25. Lumeng CN, Deyoung SM, Bodzin JL, Saltiel AR. Increased inflammatory properties of adipose tissue macrophages recruited during diet-induced obesity. Diabetes. 2007; 56(1):16–23. Epub 2006/12/29. doi: 10.2337/db06-1076 PMID: 17192460

26. Lumeng CN, Deyoung SM, Saltiel AR. Macrophages block insulin action in adipocytes by altering expression of signaling and glucose transport proteins. Am J Physiol Endocrinol Metab. 2007; 292(1):E166–74. Epub 2006/08/24. doi: 10.1152/ajpendo.00284.2006 PMID: 16926380

27. Morris DL, Singer K, Lumeng CN. Adipose tissue macrophages: phenotypic plasticity and diversity in lean and obese states. Curr Opin Clin Nutr Metab Care. 2011; 14(4):341–6. Epub 2011/05/19. doi: 10.1097/MCO.0b013e328347970b PMID: 21587064

28. Odegaard JI, Ricardo-Gonzalez RR, Red Eagle A, Vats D, Morel CR, Goforth MH, et al. Alternative M2 activation of Kupffer cells by PPARdelta ameliorates obesity-induced insulin resistance. Cell Metab. 2008; 7(6):496–507. Epub 2008/06/05. doi: 10.1016/j.cmet.2008.04.003 PMID: 18522831

29. Odegaard JI, Chawla A. Alternative macrophage activation and metabolism. Annu Rev Pathol. 2011; 6:275–97. Epub 2010/11/03. doi: 10.1146/annurev-pathol-011110-130138 PMID: 21034223

30. Ortega MT, Xie L, Mora S, Chapes SK. Evaluation of macrophage plasticity in brown and white adipose tissue. Cell Immunol. 2011; 271(1):124–33. Epub 2011/07/16. doi: 10.1016/j.cellimm.2011.06.012 PMID: 21757190

31. Schmittgen TD, Livak KJ. Analyzing real-time PCR data by the comparative C(T) method. Nature protocols. 2008; 3(6):1101–8. Epub 2008/06/13. PMID: 18546601

32. Lumeng CN, DelProposto JB, Westcott DJ, Saltiel AR. Phenotypic switching of adipose tissue macrophages with obesity is generated by spatiotemporal differences in macrophage subtypes. Diabetes. 2008; 57(12):3239–46. doi: 10.2337/db08-0872 PMID: 18829989

33. Gaillard R, Rifas-Shiman SL, Perng W, Oken E, Gillman MW. Maternal inflammation during pregnancy and childhood adiposity. Obesity (Silver Spring). 2016; 24(6):1320–7.

34. Tuchscherer M, Otten W, Kanitz E, Grabner M, Tuchscherer A, Bellmann O, et al. Effects of inadequate maternal dietary protein:carbohydrate ratios during pregnancy on offspring immunity in pigs. BMC Vet Res. 2012; 8:232. doi: 10.1186/1746-6148-8-232 PMID: 23190629

35. Cox AR, Gottheil SK, Arany EJ, Hill DJ. The effects of low protein during gestation on mouse pancreatic development and beta cell regeneration. Pediatr Res. 2010; 68(1):16–22. doi: 10.1203/00006450-201011001-00026 PMID: 20386490

36. Straus DS, Takemoto CD. Effect of dietary protein deprivation on insulin-like growth factor (IGF)-I and -II, IGF binding protein-2, and serum albumin gene expression in rat. Endocrinology. 1990; 127(4):1849–60. Epub 1990/10/01. doi: 10.1210/endo-127-4-1849 PMID: 1698149

37. Woods LL, Ingelfinger JR, Rasch R. Modest maternal protein restriction fails to program adult hypertension in female rats. Am J Physiol Regul Integr Comp Physiol. 2005; 289(4):R1131–6. Epub 2005/06/18. doi: 10.1152/ajpregu.00037.2003 PMID: 15961538

38. Sathishkumar K, Elkins R, Yallampalli U, Yallampalli C. Protein restriction during pregnancy induces hypertension in adult female rat offspring–influence of oestradiol. Br J Nutr. 2012; 107(5):665–73. doi: 10.1017/S0007114511003448 PMID: 21787449

39. Sathishkumar K, Elkins R, Yallampalli U, Yallampalli C. Protein restriction during pregnancy induces hypertension and impairs endothelium-dependent vascular function in adult female offspring. J Vasc Res. 2009; 46(3):229–39. doi: 10.1159/000166390 PMID: 18957856

40. Langley SC, Jackson AA. Increased systolic blood pressure in adult rats induced by fetal exposure to maternal low protein diets. Clin Sci (Lond). 1994; 86(2):217–22; discussion 121.

41. Gangula PR, Reed L, Yallampalli C. Antihypertensive effects of flutamide in rats that are exposed to a low-protein diet in utero. Am J Obstet Gynecol. 2005; 192(3):952–60. doi: 10.1016/j.ajog.2004.09.008 PMID: 15746697

42. Lumeng CN, Bodzin JL, Saltiel AR. Obesity induces a phenotypic switch in adipose tissue macrophage polarization. J Clin Invest. 2007; 117(1):175–84. Epub 2007/01/04. doi: 10.1172/JCI29881 PMID: 17200717

43. Guan H, Arany E, van Beek JP, Chamson-Reig A, Thyssen S, Hill DJ, et al. Adipose tissue gene expression profiling reveals distinct molecular pathways that define visceral adiposity in offspring of maternal protein-restricted rats. Am J Physiol Endocrinol Metab. 2005; 288(4):E663–73. doi: 10.1152/ajpendo.00461.2004 PMID: 15562247

44. Weisberg SP, McCann D, Desai M, Rosenbaum M, Leibel RL, Ferrante AW Jr. Obesity is associated with macrophage accumulation in adipose tissue. J Clin Invest. 2003; 112(12):1796–808. doi: 10.1172/JCI19246 PMID: 14679176

45. Berends LM, Fernandez-Twinn DS, Martin-Gronert MS, Cripps RL, Ozanne SE. Catch-up growth following intra-uterine growth-restriction programmes an insulin-resistant phenotype in adipose tissue. Int J Obes (Lond). 2013; 37(8):1051–7.

46. Claycombe KJ, Uthus EO, Roemmich JN, Johnson LK, Johnson WT. Prenatal Low-Protein and Postnatal High-Fat Diets Induce Rapid Adipose Tissue Growth by Inducing Igf2 Expression in Sprague Dawley Rat Offspring. J Nutr. 2013. Epub 2013/08/16.

47. Tarry-Adkins JL, Chen JH, Jones RH, Smith NH, Ozanne SE. Poor maternal nutrition leads to alterations in oxidative stress, antioxidant defense capacity, and markers of fibrosis in rat islets: potential underlying mechanisms for development of the diabetic phenotype in later life. Faseb J. 2010; 24 (8):2762–71. Epub 2010/04/15. doi: 10.1096/fj.10-156075 PMID: 20388698